CEMENT COMPOSITES WITH WASTE INCORPORATION UNDER ACID RAIN ATTACK

Adriana Estokova *, Robert Figmig and Nikola Galanova

Technical University of Košice, Faculty of Civil Engineering, Vysokoskolska 4, Kosice 042 00, Slovakia

ABSTRACT
The paper is aimed at the study of the resistance of cement pastes containing various secondary materials (fly ash, zeolite, zeoslag, slag and microsilica) in the model environment of acid rain. Changes in characteristics of the studied materials due to acid rain, such as compressive strength of cement composites, water absorption, penetration of aggressive ions, pH of material and its chemical composition were analysed. Model acidic environments represented solutions simulating acid rain with different pH values (2, 4 and 6). Natural acid rain, deionized water and saturated solution of $Ca(OH)_2$ were used as reference media. Based on the experimental findings, it can be stated that a positive effect of the secondary materials on increasing the resistance of cement pastes has been proven. The cement pastes with added additives resulted in a significant reduction in permeability in each model environment. This fact has an impact on the overall durability due to the fact that the amount of aggressive ions in the internal structure is reduced, causing corrosion and subsequent deterioration of cement composites. Based on the innovative methodology for the ion-penetration test of cement pastes, a coefficient was designed, which characterizes the effect of the used admixture in terms of pozzolanic resp. latent hydraulic activities. Based on this coefficient, the most significant positive effect was manifested by the use of an admixture of ash and zeolite. The rapid chloride penetration (RCP) test method has thus proved to be much more relevant in comparison with, for example, water absorption.

1. INTRODUCTION

Construction is one of the sectors that contributes significantly to the pollution of the environment in which we live (IPPC 2007). In addition to the production of high emissions of greenhouse and acidifying gases, the depletion of raw material resources and the generation of waste are also associated with this sector (Megdal 2018, Asif et al. 2007). One of the ways to reduce the mentioned negative environmental impacts and apply the principles of sustainability in construction is to try to extend the life of structures and buildings by increasing the durability of building materials (Pietrucha-Urbanik et al. 2019). Acid rain, which is caused by heavy air pollution, is currently a pretty big problem not only for people, but also for the materials that this rain affects. Therefore, it is especially important to pay attention to what material is used to withstand this effect.

The problem of acid corrosion has been addressed by several authors, paying particular attention to laboratory experiments where the effects of acid rain on cement composites were studied by immersion tank or spray tests using laboratory-prepared acid solutions simulating natural acid rain. Zeng et al. (2020) investigated the effect of acid rain on emulsified cement-asphalt mortar, which is used in China as a basic building block in railway construction. Zhihong (2017) et al. studied the deterioration of strength characteristics of concrete composites, based on ordinary Portland cement, due to the action of a simulated acid rain solution with different pH values (1.5, 2.5 and 3.5). The results showed that the action of acid rain caused surface disturbance and gradual crushing of concrete materials. Other authors (Shaodong Xie et al. 2004, Fan et al. 2010) dealt mainly with the confirmation of the positive effects of various pozzolanic admixtures on increasing the resistance of cement composites to acid rain using accelerated laboratory tests. The authors found that cement composites with slag cement and fly ash were more resistant than composites with ordinary Portland cement due to changes in compressive strength values. In addition, the experimental results showed that the corrosion rate was higher when soaking the samples compared to spraying the acidic solution. The rate of weight loss increased gradually with increasing immersion time of the sample. The changes were more significant for samples exposed to pH 1.5 solutions

than for samples in pH 2.5 and 3.5 solutions. The influence of nanosilicates, as another mineral admixture, on the properties of cementitious materials under acid rain conditions was studied in (Mahdikhani, 2018). The nanosilicates proved their positive effects on the mechanical properties and durability of concrete samples. The attention was paid also on monitoring the effects of acid rain on the filler component of concrete. Caifeng Lu et al. (2020) dealt with changes in the mechanical properties of recycled aggregate concretes due to acid rain. The authors confirmed that the appropriate addition of fly ash and silica fume increased strength and resistance to acid rain, while higher replacement of recycled aggregates appeared to be unfavourable as these samples were less resistant to acid rain.

The main objective of this work was to compare the resistance of cement pastes containing waste and mineral admixtures of fly ash, zeolite, zeoslag, slag and microsilica in order to increase their resistance in the model environment of acid rain. The novelty of the work was in applying the ion-penetration test to assess the durability of particular pastes based on the new proposed permeability reduction coefficient.

2. MATERIALS AND METHODS

2.1 Pastes with secondary materials

For the study of acid rain attack, 5 different types of cement pastes were produced. The ordinary Portland cement CEM I 42.5 R (CRH, Turňa nad Bodvou, Slovakia) was used in the pastes and part of the cement was replaced by secondary raw materials and wastes, which are recommended as a measure to increase the resistance of composites in acidic environments. The chemical composition of cement and individual secondary materials, studied by XRF analysis, are given in Table 1. The specific densities of materials were as followed: 3050, 2440, 2900, 2200, and 2800 kg/m^3 for cement, zeolite, zeoslag, microsilica, and fly ash, respectively. The sizes of materials, represented by the average grain, were in the interval 15.1 to 36.3 micrometers.

Microsilica and zeolite as pozzolanic materials have a significantly higher proportion of SiO_2 than CaO, while zeoslag with a predominant amount of blast furnace slag has a high CaO content.

In particular cement pastes samples, a 15% of cement was substituted by zeolite (Zeocem, Bystré, Slovakia), microsilica (Mapeplast, Mapei, Slovakia), combination of zeolite and slag (Zeobau 50 - 80% slag and 20% zeolite) and fly ash (TEKO, Košice, Slovakia) – Table 2. The recipes of the cement samples were set to the water-to-binder ratio (w/b) of 0.45 as required per the extremely aggressive acidic environment (XA3 class) according to the standard EN 206-1 (2013, 2021).

Cement pastes were prepared in the form of cubes (40 × 40 × 40) mm and beams with dimensions of 40 × 40 × 160 mm. Reference samples were made in two ways, where C0 was the very first setting target. C0 was made with a hand mixer and the sample, marked C1, was made in a standard mixer. Materials were slowly mixed for 150 s, and after 60-second pause, the mixing was continued for another 150-second period. The cement material was put into the molds, vibrated for 5 s and covered by impermeable foil to prevent specimen from drying out. After demoulding, the

TABLE 1: XRF analysis of materials.

	Concentration of the elements expressed in oxide form (wt. %)				
Oxides	**Cement**	**Microsilica**	**Zeolite**	**Fly ash**	**Zeoslag**
MgO	1.19	1.07	1.18	2.64	8.32
Al_2O_3	4.14	0.36	14.14	21.38	9.49
SiO_2	20.37	92.46	71.96	44.00	45.55
P_2O_5	0.50	0.05	0.05	0.28	0.04
SO_3	6.96	0.07	0.01	0.23	0.46
Cl	0.11	0.14	0	0	0.02
K_2O	1.10	0.99	2.27	2.13	0.84
CaO	61.88	0.27	3.16	5.89	32.27
TiO_2	0.22	-	0.51	1.90	0.40
MnO	0.04	0.58	0.03	0.14	0.59
Fe_2O_3	2.67	1.24	3.61	12.35	1.15

TABLE 2: Cement pastes composition and labeling.

Cement paste sample	Labelling	Cement content (g)	Water content (g)	Secondary material (g)	w/b
Reference sample	C0, C1	3850	1732.5	-	0.45
Paste with zeolite	Z	3272.5	1732.5	577.5	0.45
Paste with microsilica	MS	3272.5	1732.5	577.5	0.45
Paste with zeoslag	ZS	3272.5	1732.5	577.5	0.45
Paste with fly ash	P	3272.5	1732.5	577.5	0.45

samples were cured in Ca(OH)$_2$ solution for 28 days and then each sample was labelled, dried to constant weight and its final weight was recorded. The saturated solution of Ca(OH)$_2$ was used to avoid the process of leaching of portlandite during the curing period of the samples.

2.2 Model experiment of acidic corrosion

The corrosion resistance experiment on cement pastes was performed as a tank test through immersing the samples in model acidic media (Table 3), over a period of 5 months whereas the pH of the liquid phases was regularly adjusted to baseline. The volume of the test medium was calculated as ten times the volume of the cement sample. The samples were immersed in plastic containers covered with lids.

6 types of model environments with different pH values were designed, which represented different acidity of the environment as well as a reference alkaline environment. A saturated solution of calcium hydroxide (Ca(OH)$_2$) was chosen as reference medium, where the process of leaching or acid corrosion was not expected. The local natural rain was collected during the period of two weeks in plastic container. Laboratory solutions of model acid rain were prepared by mixing of corresponding solutions of 93% sulphuric acid and 65% nitric acid in a ratio of 6:4 to resemble the basic composition of acid rain as much as possible (Zabawi 2008). The action of ions other than sulphates and nitrates present in natural rain has not been studied.

2.3 Analytical procedures

Several parameters were studied on cement composites before and after the experiments: bulk density of samples, changes in weight and water absorption, penetration of aggressive ions, compressive strength tests, and the pH of the cement pastes and corrosive media. The results of the parameters tested are presented as an average of two measurements.

Consistency of fresh pastes was investigated according to EN 1015-3 (2007), where the average value of the cake formed was measured in time of 5 minutes after first contact of binder and water (zero time) on Haegerman table and then after 25 strikes.

Two methods were used to determine the bulk density. Water immersion measurement using cylinder with an aspect ratio of 1: 2 was used for fresh cement paste. For hardened paste before the compressive strength test, di-

mensional determination based on dimensions was used.

Water absorption was determined on the basis of the masses of the dry and wet cement pastes samples (see expression 1), which were weighed on analytical balances (Radwag), with an accuracy of 3 decimal places. The cement pastes were dried in laboratory oven at temperature of 105±5°C to constant mass.

$$WA = \frac{m_w - m_d}{m_d} \cdot 100 \qquad (1)$$

where,
m$_d$ −mass of dry sample (g);
m$_w$ − mass of wet sample (g);
WA − water absorption (%).

To compare the permeability of cement pastes, the rapid chloride penetration test (RCP test) was performed, according to ASTM C1202-19. The test is based on measuring the penetration of chloride ions through the material. For each type of cement paste, two samples were tested in order to obtain a representative value. Electrolytes of 3% NaCl solution (cathode) and 0.3M NaOH solution (anode) were used for RCP testing. The voltage in the system was around 60 V and the sample was cooled during the test by a 12 V DC fan measuring 80 × 80 mm. Our measurement procedure was slightly modified so that test was performed over a period of 25-30 minutes for one test sample. The minimum and maximum current were recorded within 1 minute. After stabilization of the current value at about 15 resp. 20 minutes, two more 5-minute intervals were recorded. During the test, the temperature of the sample was measured with a non-contact IR thermometer and the electrolyte temperature was measured using temperature probes (J-type). According to passing charge result, permeability and thus the quality of cement paste can be evaluated.

Compressive strength of cement pastes was tested after 28 days of curing under saturated calcium hydroxide solution. For the final value of compressive strength, 3 samples were tested according to EN 12390 (2019) with loading speed of 0,5 MPa (equals to 0.8 kN/s).

The pH of the cement paste was determined based on the leachate of the material in a liquid medium. After the destructive compressive strength test, the samples were ground and sieved on a sieve with a size of 0.063 mm. 1 g of cement paste material was mixed with 100 ml of deionized water and stirred for 1 minute. Subsequently, a pH meter (Extech EC500) was used for pH value determination in cement samples leachate and in corrosive media as well.

The composition of the raw materials of the prepared cement pastes was analysed by the X-ray fluorescence method (XRF) using Ametec Spectro IQ analyser (Ametec, Mahwah, NJ, USA).

3. RESULTS AND DISCUSSION

3.1 Characteristics of fresh composites and hardened pastes after 28 days

3.1.1 Consistency of cement pastes

The results of the Haegerman's test measuring the flowability of the fresh cement pastes are presented in Figure 1. Replacement of cement by secondary materials

TABLE 3: Model solutions.

Medium	Labelling	pH
Ca(OH)$_2$	CH	12.5
Deionized water	DV	7.0
Natural acid rain	NR	6.5
Model acid rain – extremely aggressive environments	MAR2	2
Model acid rain – aggressive environments	MAR4	4
Model acid rain – slightly aggressive environments	MAR6	6

(microsilica, zeoslag and fly ash) had no significant effect on the consistency. The initial consistency of MS, ZS and P samples ranged from 170 to 188 mm while the initial consistency of reference sample was 176 mm. However, partial replacement of cement by zeolite led to decreasing in consistency of cement paste (137 mm). This may be due to the clathrate structure of the zeolite crystal lattice, which causes water to bind to the space in the middle of the host cluster (Martínez and Corma 2013).

3.1.2 Bulk density

The bulk density of the cement composite decreased with the addition of an admixture, which is due to the different bulk densities of the input materials (Figure 2). The highest values are reached by reference samples C0 and C1, where the maximum values of bulk densities of samples in the saturated state (D-ssd) were about 1984 kg.m^{-3}. This was the same for dry samples (D-28-dry), the highest values were also reached by reference samples C0 and C1. The D-mix in the figure represents the bulk density of the fresh paste after mixing. The measured values of bulk densities of cement pastes are comparable with those determined by Allahverdi et al. (2010) but lower than reported by Heikal et al. (2020) who investigated the pastes with clay nanoparticles.

3.1.3 Water absorption and weight changes

After 28 day-curing in the reference medium $Ca(OH)_2$, the weights of the samples were measured in wet and dry state to obtain the water absorption. The highest water absorption of 28.8% was reached by the sample with the admixture of fly ash (P), however, this was very close to the absorption of sample with a combination of zeolite and slag (ZS). Samples with an admixture of zeolite (Z) and microsilica (MS) achieved the lowest absorption as seen in Table 4. Allahverdi, on the contrary found that microsilica addition contribute to the increase in water absorption of the pastes.

3.1.4 Compressive strength

The highest value of compressive strength after 28 days was reached by reference samples C0 and C1, up to 63.8 MPa (Table 5). The lowest compressive strength was achieved by a sample with an admixture of fly ash (P), namely 52.5 MPa which was consistent with the study conducted by Wang et al. (2016). However, the pozzolanic properties of the fly ash and the latent hydraulic properties of the zeoslag may not have been exhibited after such a short time, as they need a longer reaction time.

3.1.5 Penetration of aggressive ions

Figure 3 shows the measured values of the current
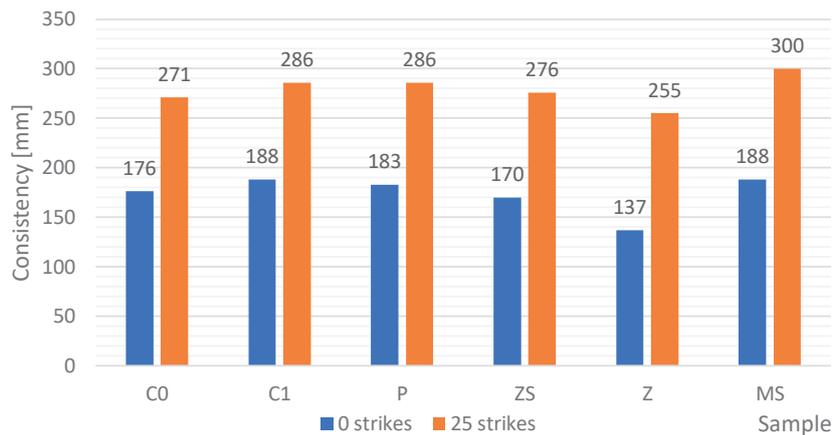
FIGURE 1: Consistency of cement pastes.
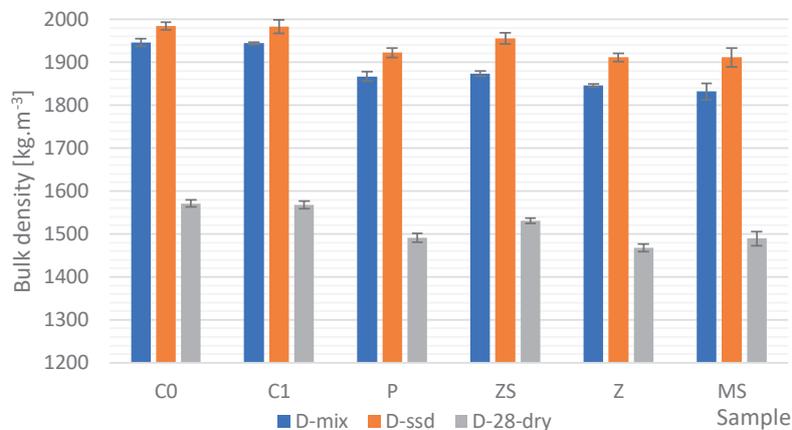
FIGURE 2: Bulk densities of cement pastes.

TABLE 4: Water absorption of cement pastes.

Cement paste sample	Water absorption value (%)		
	Average	Standard deviation	Variation
C0 - reference	26.2	0.3	1.0
C1 - reference	26.9	0.5	1.9
P – with fly ash	28.8	0.6	2.1
ZS – with zeoslag	28.6	0.1	0.3
Z – with zeolite	25.4	0.2	0.8
MS – with microsilica	24.9	0.4	1.8

TABLE 5: Compressive strength of cement pastes.

Cement paste sample	Compressive strength (MPa)		
	Average	Standard deviation	Variation
C0 - reference	61.6	1.8	2.9
C1 - reference	63.8	3.5	5.5
P – with fly ash	52.5	1.9	3.6
ZS – with zeoslag	54.6	2.6	4.7
Z – with zeolite	61.5	1.7	2.7
MS – with microsilica	56.0	1.6	2.9

passing through the individual cement pastes at the beginning of the measurement (I-0), as well as the maximum current passed (I-max), which were recorded for the cement pastes. The higher current represents a larger amount of ions penetrating into the structure of the cement paste and thus its lower ability to withstand aggressive environments. The highest values of ion penetration (0.6 A) were recorded in the sample with the addition of fly ash. The composite with microsilica reached the lowest value - 0.36 A, due to its admixture, because it acted as a filler and thus blocked the passage of ions through the

sample. In comparison with the compressive strengths values of the samples presented in Figure 3, it can be seen that the values of the ion penetration corresponded to the values of the compressive strengths, where the fly ash reached the lowest value.

3.1.6 pH of cement pastes

The measured pH values of cement paste samples, determined after 28 days of samples curing, are compared in Figure 4. The highest pH values, 13 and 12.8, were observed for the reference samples C0 and C1, respective-
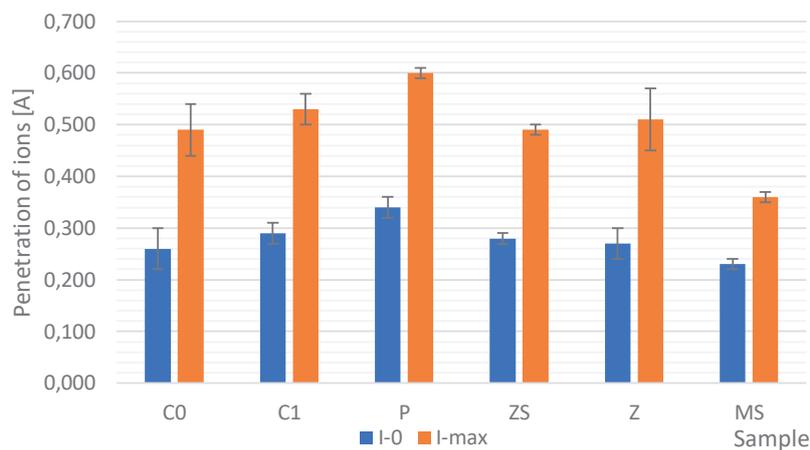
FIGURE 3: Results of the RCP test of cement pastes before the corrosion experiment..
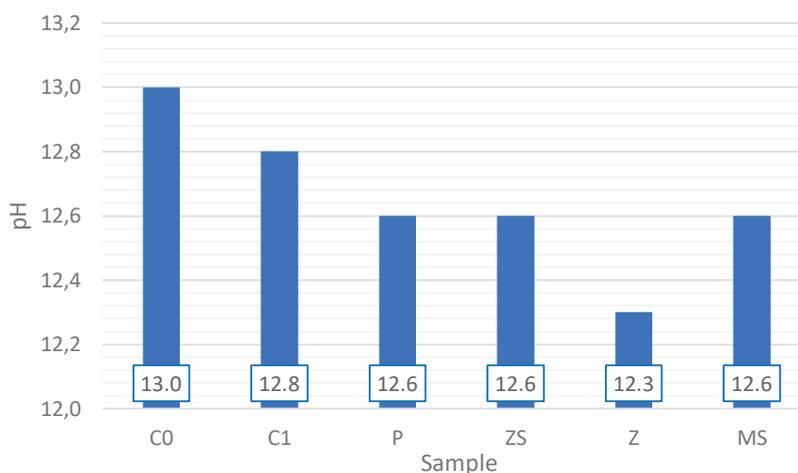
FIGURE 4: pH of the cement paste samples.

ly. The lowest value was measured in a sample of cement paste with zeolite (Z), where the pH reached 12.3.

3.2 Properties of cement pastes after exposure in model solutions

3.2.1 Increase in bulk density

After the experiment, there was noticed an increase in bulk densities (D-ssd) for most cement pastes after their exposure to a corrosive model environment. In deionized water (DV) and in natural rain (NR), the increase in the bulk density of the samples was very similar and in comparison with other environments neglible (0.05 - 0.6%) – Figure 5 b) and c). This result is related to the fact that the environment of natural rain was very similar to the environment of deionized water not only in terms of acidity, but also due to its low conductivity and minimal presence of sulphates. The changes in the bulk densities of the samples in the environments with model acid rain were several times higher, as can be seen in Figure 5 d) - f). The increase in the bulk density of the samples in an aggressive environment
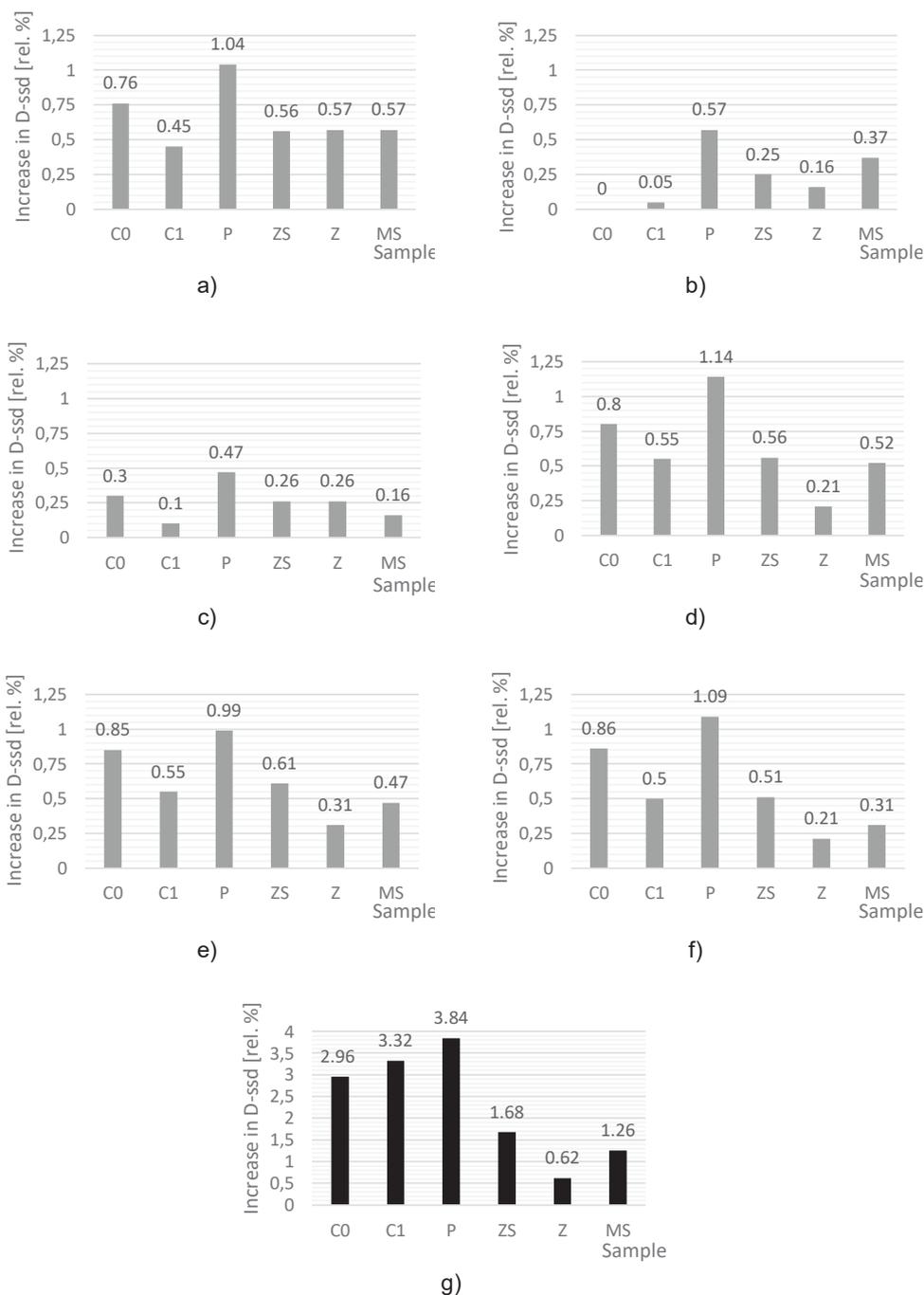
FIGURE 5: Changes in bulk densities of cement pastes after exposure to a) Ca(OH)2 reference medium, b) deionized water, c) natural acid rain, d) model acid rain with pH = 6, e) model acid rain with pH = 4, f) model acid rain with pH = 2, g) model acid rain pH = 2 – samples with precipitates.

is probably associated with the formation of new sulphate compounds not only on the surface of the sample, but also with their crystallization in the internal structure (Rozière et al. 2009; Zhang et al. 2013). These sulphate compounds were formed as a result of the presence of sulphate ions in the aggressive solution. Sulphates likely reacted with calcium ions, either directly leached in a liquid medium or even after penetrating inside of a paste with not yet leached portlandite. On the contrary, the increase in the bulk density of cement pastes in the reference environment $Ca(OH)_2$, where corrosion did not occur by leaching portlandite, is probably related to the ongoing hydration processes. The highest increase in bulk density was recorded for a sample of cement paste with fly ash (P).

3.2.2 Water absorption changes

A comparison of the water absorption (WA) of cement paste samples before (orange) and after the corrosion experiment (blue) is shown in Figure 6.

In the reference medium, the absorption values of all samples except the zeolite and microsilica pastes decreased compared to the 28-day absorption, likely due to ongoing hydration processes as the pores were filled with hydration products (Moghadam et al 2020). For samples immersed in deionized water, the absorption was approximately the same as at the beginning of the experiment, but for the zeolite (Z) and microsilica (MS) samples, an increase in absorption was again observed. Similar trends in absorption as in deionized water were observed for cement samples immersed in natural acid rain (Figure 6 c). The values reached for the reference samples and zeoslag-based samples were lower than the original ones. The value of the cement paste with fly ash increased slightly. Absorption values of Z and MS samples increased significantly. The increase in absorption in water and natural rain could be linked with the portlandite leaching from the cement matrix (Jebli et al. 2018, Carde et al. 1996). Samples in MAR6 and MAR4 media behaved the same, the values remained
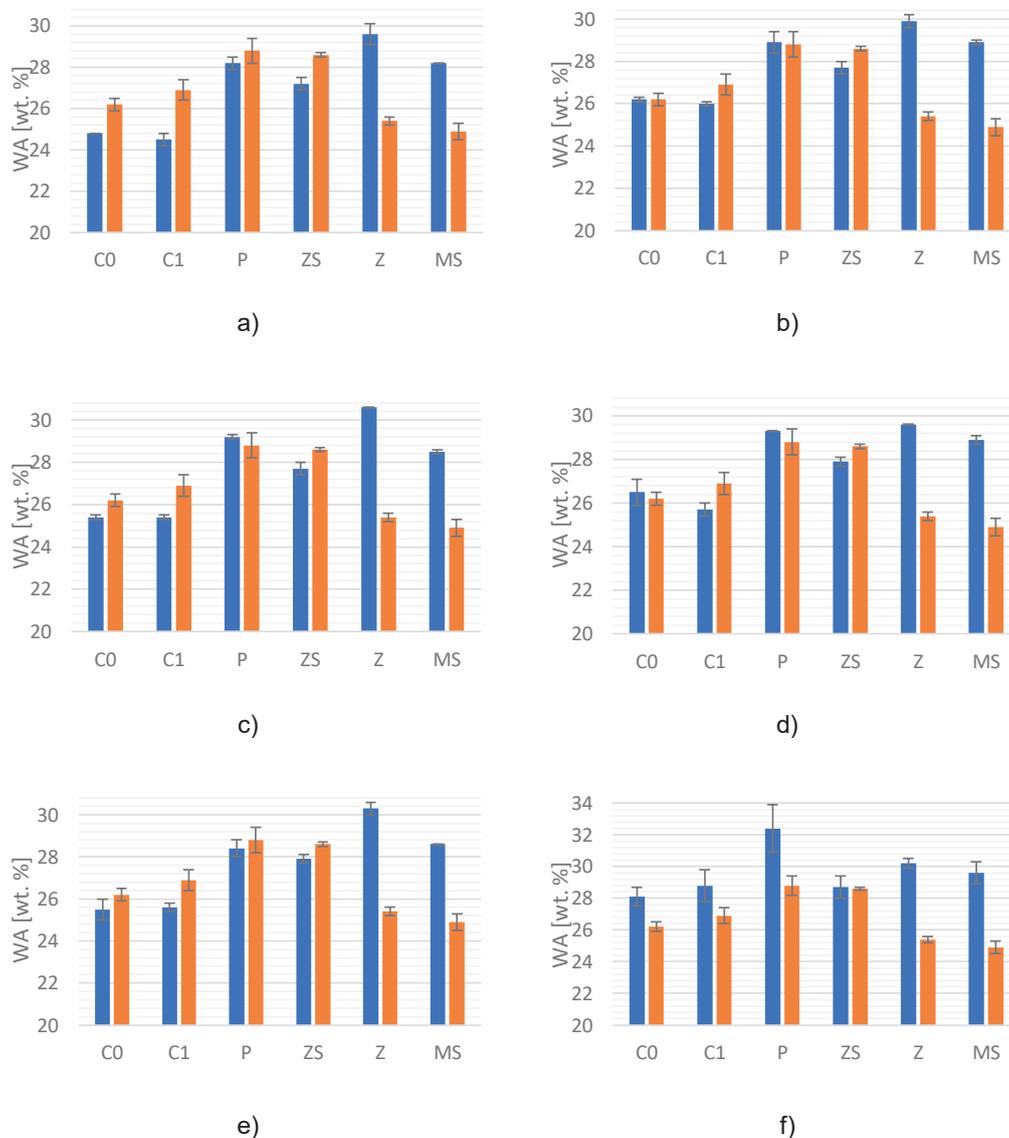
FIGURE 6: Comparison of absorption of cement pastes before and after exposure to a) reference medium Ca(OH)2, b) deionized water, c) natural acid rain, d) model acid rain with pH = 6, e) model acid rain with pH = 4, f) model acid rain with pH = 2.

at the original level, but the values for Z and MS increased. The solution of model acid rain with pH 2 was confirmed as clearly the most aggressive, in which the values after the absorption experiment increased in all samples compared to the original absorption.

The absorption of the most of samples changed only minimally due to experiment, but this was not the case for samples Z and MS. After the experiment, all pastes with zeolite and microsilica achieved higher values of absorption than the original ones. This indicates their lower resistance compared to fly ash and zeoslag pastes.

3.2.3 pH of aggressive media

The pH values of liquid experimental media of cement pastes with fly ash addition (P sample - on the left) and reference sample (C0 – on the right) are illustrated in Figure 7. As seen in Figure 7, the pH values raised dramatically in the corrosion experiment after samples immersing and reached the values above 11. The increase in pH of the media was linked to the cement components leaching, mainly of portlandite $(Ca(OH)_2)$, which contributed to the higher concentrations of hydroxide ions (Beddoe et al. 2022). This finding is in correlation with the other authors and our previous research as well (Zhou et al. 2018, Estokova et al. 2018, Rozière et al. 2009). During whole experimental period, the pH fluctuated in the interval of 11-12, in spite of the fact that the pH was regularly set to the initial value. This confirmed the observation, that the leaching of the cement matrix was in progress during the whole experiment. The very similar values in pH during the exposition of samples to the various media led to the conclusion, that process of dissolution of the hydration components in cement pastes dominated in the experiment. The trends in pH for the other samples were similar to those of presented.

3.2.4 Change in permeability of pastes determined by RCP test

In every model solution, each sample achieved a lower ion penetration after the experiment compared to the penetration before, which was manifested by a decrease in permeability for each sample (Figure 8).

In the case of cement pastes immersed in DV, CH and VD, this phenomenon was probably related to the ongoing hydration process, which probably dominated the processes of leaching of basic components. Yang et al. (2018) reported that leaching by deionized water is a very slow process and it is limited by calcium concentration in the pore solution higher than 20 mol/m³. In the case of cement pastes, which were immersed in model acid rain solutions, the reduction in the permeability of the samples was additionally affected by the formation of new sulphate compounds.

The highest initial (I-0) and maximum (I-max) current values measured for cement pastes after corrosion experiments were observed in reference samples C0 and C1. This means that in these samples, the highest penetration of aggressive ions was identified. On the contrary, in the samples with fly ash (P) and zeolite (Z) the values of ion penetration were the lowest, which in the case of cement pastes with fly ash also correlates with the results of water absorption.

Based on the measured values of ion penetration through cement pastes, the coefficient of reduction of permeability (KPR) was proposed to compare the efficiency of adding mineral admixtures (Expression 2). This coefficient was designed on the basis of comparing the values of measured maximum currents of individual samples of cement pastes with the reference sample C0.

$$KPR = 100 - \left(\left(\frac{I - \max(P_p)}{I - \max(C0_p)} \right) \times 100 \right) \quad (\%) \quad (2)$$

where KPR is permeability reduction coefficient; $I\text{-}\max(P_p)$ is the measured value of I-max of the particular cement paste in the model solution p; and $I\text{-}\max(C0_p)$ is the measured value of I-max of the reference sample in the model solution p.

A comparison of the contributions of individual mineral admixtures to reduce the overall permeability of the sample and thus to increase its resistance in the studied envi-
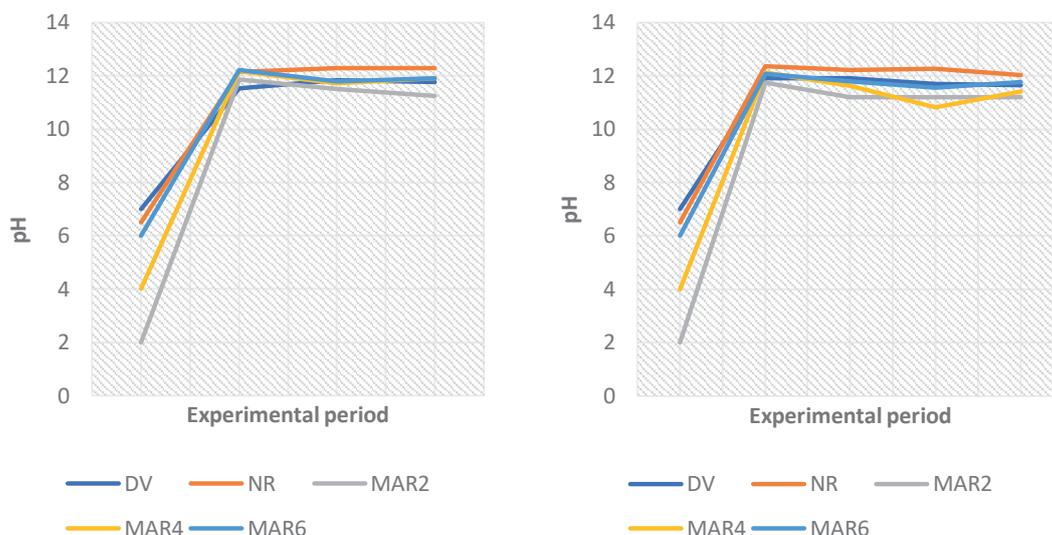
FIGURE 7: The pH trends of experimental media of samples P (left) and C0 (right).

a)

b)

c)

d)

e)
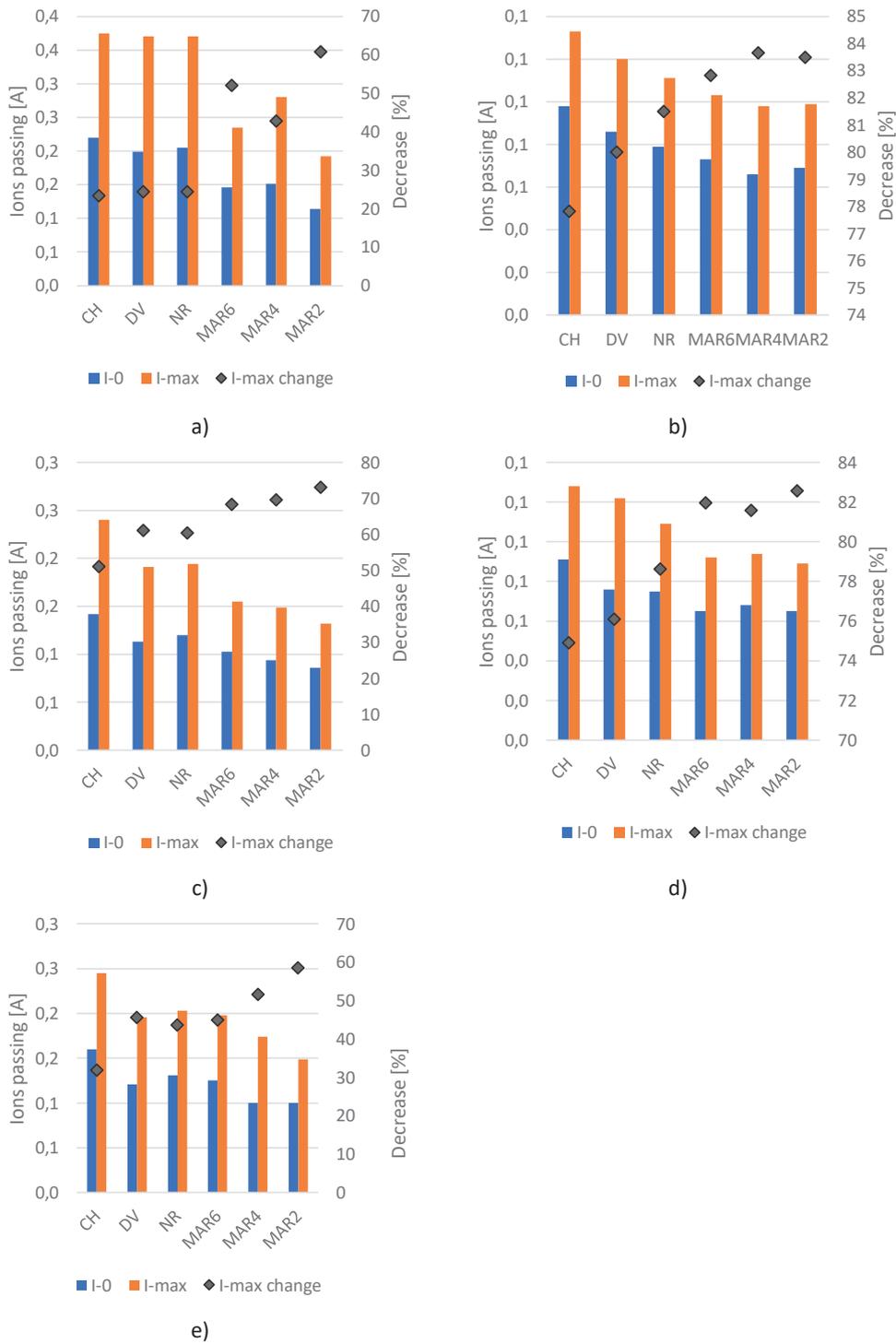
FIGURE 8: Measured I-0 and I-max of cement pastes after the experiment compared to the input values for a) C0 sample, b) P sample, c) ZS sample, d) Z sample, e) MS sample.

ronments is shown in Figure 9.

The more aggressive the environment, the less positive effect of the admixture was manifested. The most effective influence of mineral admixtures was found in the model solutions of natural rain and deionized water. As seen in Figure 5, the use of any admixture reduces the permeability of the cement paste, but the best results have been obtained by adding fly ash (P) or zeolite (Z).

3.2.5 Visual changes of cement samples

Various precipitates were observed on the surface of the cement paste samples after the acid rain exposure. The precipitates were mostly white and occurred predominantly on samples immersed in the MAR2 acid rain model solution. Figure 10 illustrates the surface of the samples that were in a model rain environment with pH = 2. The new-formed surface compounds are likely based on

the sulphates (Malolepsy et al. 2015, Zhang et al. 2013, García-Vera et al. 2018, Estokova et al. 2016).

In addition to surface precipitates, visible damage in the form of surface cracks as well as complete disintegration of the sample was observed for the samples of cement pastes, which were exposed in the model environment with pH = 2.

4. CONCLUSIONS

In this work, the effect of acid rain causing acidic, sulphate and leaching corrosion was studied on cement pastes with various mineral admixtures. Cement pastes with added additives based on waste and supplementary cementitious materials resulted in a significant reduction in permeability in each model solution. Based on the RCP test, an innovative approach was designed to evaluate the effect of the particular admixtures on the improving of permeability of the cement pastes, in terms of their pozzolanic and latent hydraulic activities. Results revealed that the most significant positive effect was manifested by the

use of admixtures of ash and zeolite. The RCP testing of the pastes has thus proved to be much more consistent in comparison with, for example, water absorption testing when comparing the influence of the individual admixtures.

REFERENCES

Allahverdi, A., Salem, S., 2010. Simultaneous influences of microsilica and limestone powder on properties of portland cement paste. Ceramics − Silikáty 54 (1) 65-71.

Asif, M., Muneer, T., Kelley, R., 2007. Life cycle assessment: A case study of a dwelling home in Scotland. Build. Environ. 42(3), 1391–1394. https://doi.org/10.1016/j.buildenv.2005.11.023

ASTM C1202-19: Standard Test Method for Electrical Indication of Concrete's Ability to Resist Chloride Ion Penetration

Beddoe, R.E., Müllauer, W., Heinz, D., 2022. On leaching mechanisms of major and trace elements from concrete - Carbonation, exposure to deicing salt and external sulphates. J. Build. Eng., 45, 103435. https://doi.org/10.1016/j.jobe.2021.103435
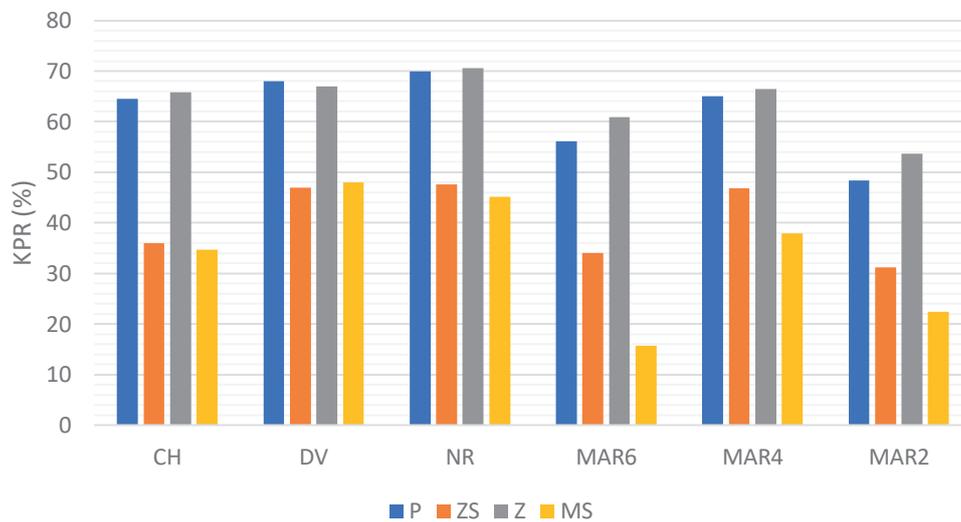
FIGURE 9: Comparison of KPRs of cement pastes.

FIGURE 10: Samples exposed to MAR2 environment a) P sample, b) MS sample.

Carde, C., François, R., Torrenti, J. M., 1996. Leaching of both calcium hydroxide and C-S-H from cement paste: Modeling the mechanical behavior, Cem. Concr. Compos. 26, 1257-1268. https://doi.org/10.1016/0008-8846(96)00095-6.

EN 1015-3:2000/A2:2007 Methods of test for mortar for masonry - Part 3: Determination of consistence of fresh mortar; European Committee for Standardization: Brussels, Belgium, 2007.

EN 12390-3:2019-07. Testing Hardened Concrete-Part 3: Compressive Strength of Test Specimens; European Committee for Standardization: Brussels, Belgium, 2019.

EN 206:2013+A2:2021 Concrete - Specification, performance, production and conformity; European Committee for Standardization: Brussels, Belgium, 2021.

Estokova, A., Kovalcikova, M., Luptakova, A., Prascakova, M., 2016. Testing silica fume-based concrete composites under chemical and microbiological sulfate attacks. Materials 9, 324. https://doi.org/10.3390/ma9050324

Estokova, A., Smolakova, M., Luptakova, A., 2018. Calcium Extraction from Blast-Furnace-Slag-Based Mortars in Sulphate Bacterial Medium. Buildings 8(1), 9. https://doi.org/10.3390/buildings8010009

Fan, Y.F., Hu, Z.Q., Zhang, Y.Z., Liu, J.L., 2010. Deterioration of compressive property of concrete under simulated acid rain environment, Constr. Build. Mater., 24(10), 1975−1983. https://doi.org/10.1016/j.conbuildmat.2010.04.002

García-Vera, V.E. et al., 2018. Exposing sustainable mortars with nanosilica, zinc stearate, and ethyl silicate coating to sulfuric acid attack. Sustainability 10, 3769. https://doi.org/10.3390/su10103769

Heikal, M., Helmy, I.M., Awad, S., Ibrahim, N.S., 2020. Improvement of cement pastes composite properties containing clay nanoparticles. Ceramics-Silikáty 64(4), 398−406. https://10.13168/cs.2020.0027

Huang, Q., Zhu, X., Liu, D., Zhao,L., Zhao, M., 2021. Modification of water absorption and pore structure of high-volume fly ash cement pastes by incorporating nanosilica. Journal of Building Engineering, 33, 101638.https://doi.org/10.1016/j.jobe.2020.101638

IPCC, 2007. Summary for Policymakers. In: Climate Change 2007: The Physical Science Basis. Contribution of Working Group I to the Fourth Assessment Report of the Intergovernmental Panel on Climate Change [Solomon, S., D. Qin, M. Manning, Z. Chen, M. Marquis, K.B. Averyt, M.Tignor and H.L. Miller (eds.)]. Cambridge University Press, Cambridge, United Kingdom and New York, NY, USA

Jebli, M., Jamin, F., Pelissou, C., Malachanne, E., Garcia-Diaz, E., 2018. Leaching effect on mechanical properties of cement-aggregate interface. Cem. Concr. Compos. 87, 10 - 19. https://doi.org/10.1016/j.cemconcomp.2017.11.018

Lu, C., Wang, W., Zhou, Q., Wei, S., Wang, C., 2020. Mechanical behavior degradation of recycled aggregate concrete after simulated acid rain spraying. J. Clean. Prod., 262, 121237.https://doi.org/10.1016/j.jclepro.2020.121237

Lu, C., Wang, W., Zhou, Q., Wei, S., Wang, C., 2021. Freeze-thaw resistance of recycled aggregate concrete damaged by simulated acid rain. J. Clean. Prod., 280, 124396. https://doi.org/10.1016/j.jclepro.2020.124396

Mahdikhani, M., Bamshad, O., Shirvani, M.F., 2018. Mechanical properties and durability of concrete specimens containing nano silica in sulfuric acid rain condition. Constr. Build. Mater. 167, 929−935. https://doi.org/10.1016/J.CONBUILDMAT.2018.01.137

Malolepsy, J., Grabowska, E., 2015. Sulfate attack resistance of cement with zeolite additive. Procedia Engineering 108, 170-176. https://doi.org/10.1016/j.proeng.2015.06.133.

Martínez, C., Corma, A., 2013. 5.05 − Zeolites, Comprehensive Inorganic Chemistry II (Second Edition). Elsevier, p. 103-131.

Megdal, S.B., 2018. Invisible water: the importance of good groundwater governance and management. NPJ. Clean Water 1(1), 1−5. https://doi.org/10.1038/s41545-018-0015-9

Moghadam, H.A., Mirzaei, A., Dehghi, Z.A., 2020. The relation between porosity, hydration degree and compressive strength of Portland cement pastes in the presence of aluminum chloride additive. Constr. Build. Mater. 250, 118884. https://doi.org/10.1016/j.conbuildmat.2020.118884Pietrucha-Urbanik, K., Studziński, A., 2019. Qualitative analysis of the failure risk of water pipes in terms of water supply safety. Engineering Failure Analysis 95, 371-378. https://doi.org/10.1016/j.engfailanal.2018.09.008

Rozière, E., Loukili, A., El Hachem, R., Grondin, F., 2009. Durability of concrete exposed to leaching and external sulphate attacks. Cement Concrete Res. 39(12), 1188-1198. https://doi.org/10.1016/j.cemconres.2009.07.021.

Wang, Z., Song, Y., 2016. Adsorption properties of CFBC ash−cement pastes as compared with PCC fly ash−cement pastes. Int J Coal Sci Technol 3, 62−67. https://doi.org/10.1007/s40789-016-0103-8

Wang, Z., Zhu, Z., Sun, X., Wang, X., 2017. Deterioration of fracture toughness of concrete under acid rain environment. Eng. Fail. Anal. 77, 76−84. https://doi.org/10.1016/j.engfailanal.2017.02.013

Xie, S., Qi, L., Zhou, D., 2004. Investigation of the effects of acid rain on the deterioration of cement concrete using accelerated tests established in laboratory. Atmos. Environ. 38, 4457−4466. https://doi.org/10.1016/j.atmosenv.2004.05.017

Yang, H., Che, Y., Leng, F., 2018. Calcium leaching behavior of cementitious materials in hydrochloric acid solution. Sci Rep 8, 8806. https://doi.org/10.1038 /s41598-018-27255-x

Zabawi, A.G., Esa, S., Leong, C.P., 2008. Effects of simulated acid rain on germination and growth of rice plant. J. Trop. Agric. and Fd. Sc., 36, 281-286.

Zeng, X., Li, Y., Ran, Y., Yang, K., Qu, F., Wang, P., 2018. Deterioration mechanism of CA mortar due to simulated acid rain. Constr. Build. Mater. 168, 1008−1015. https://doi.org/10.1016/j.conbuildmat.2018.03.033

Zhang, M.H., Chen, J.K., Lv, Y.F., Wang, D.J., Ye, J., 2013. Study on the expansion of concrete under attack of sulfate and sulfate-chloride ions. Constr. Build. Mater. 39, 26-32. https://doi.org/10.1016/j.conbuildmat.2012.05.003.

Zhou, C., Zhu, Z., Wang, Z., Qiu, H., 2018. Deterioration of concrete fracture toughness and elastic modulus under simulated acid-sulfate environment. Constr. Build. Mater. 176, 490-499. https://doi.org/10.1016/j.conbuildmat.2018.05.049